

# Solid State $^{15}\text{N}$ and $^{13}\text{C}$ NMR Study of Several Metal 5,10,15,20-Tetraphenylporphyrin Complexes

Mark Strohmeier, Anita M. Orendt, Julio C. Facelli,<sup>†</sup> Mark S. Solum,<sup>‡</sup> Ronald J. Pugmire,<sup>‡</sup> Robert W. Parry, and David M. Grant\*

Contribution from the Department of Chemistry, Department of Chemical and Fuels Engineering, and the Center for High Performance Computing, University of Utah, Salt Lake City, Utah 84112-1102

Received February 10, 1997. Revised Manuscript Received April 15, 1997<sup>⊗</sup>

**Abstract:** The principal values of both the  $^{13}\text{C}$  and  $^{15}\text{N}$  chemical shift tensors are reported for the Zn, Ni, and Mg 5,10,15,20-tetraphenylporphyrin (TPP) complexes. The principal values of the  $^{15}\text{N}$  chemical shift tensors were obtained from static powder patterns of  $^{15}\text{N}$ -enriched samples. Due to overlap between the powder patterns of the different carbons, the  $^{13}\text{C}$  values were obtained using the recently developed magic angle turning (MAT) 2D experiment on unenriched materials. The measured principal values are presented along with theoretical calculations of the chemical shift tensors and a discussion of the effects that the metal bonding has on the chemical shift tensors in these compounds. Both the isotropic chemical shift and the principal values of the  $^{15}\text{N}$  chemical shift tensor are nearly identical for the Mg and Zn complexes. The  $^{15}\text{N}$  isotropic chemical shift for the NiTPP, however, changes by nearly 80 ppm relative to the Mg and Zn values, with large changes observed in each of the three principal values. Calculations show that the differences between the  $^{15}\text{N}$  chemical shifts are almost entirely determined by the metal–nitrogen separation. In addition, both the experimental data and the calculations show only very minor differences in the  $^{13}\text{C}$  chemical shift tensor components as the metal is changed.

## Introduction

In many natural products porphyrins, metalloporphyrins, and related macrocycles form the reactive site for important biological activity.<sup>1</sup> They are also abundant in geological formations such as oils, coals, soils, etc. Thus porphyrins and related molecules have numerous applications in all fields of chemistry and in medicine. Because of this importance and their interesting chemical, physical, and biological properties, they have been widely investigated for over 100 years.

Since NMR chemical shift data can provide detailed insights into the chemical structure, NMR methods are often used in the investigation of these compounds. For example, there are numerous publications on the dynamics of the hydrogen rearrangement in various free base porphyrins, using  $^1\text{H}$ ,  $^2\text{H}$ ,  $^3\text{H}$ ,  $^{13}\text{C}$ , and  $^{15}\text{N}$  solution state NMR,<sup>2–7</sup> as well as a number of  $^{13}\text{C}$ <sup>8–10</sup> and  $^{15}\text{N}$ <sup>2,5,11</sup> solid state NMR measurements. The principal values of the  $^{15}\text{N}$  chemical shift tensor have been

measured in the free base tetraphenylporphyrin.<sup>12</sup> There are also solution  $^{13}\text{C}$  NMR studies of the effect that different metals have on the isotropic chemical shifts,<sup>13–15</sup> as well as solution and solid state measurements on the metal itself.<sup>16,17</sup> Additional studies have measured the effect the addition of ligands has on the chemical shifts of metal–porphyrin complexes.<sup>18</sup>

The measurement of the principal values of the chemical shift tensor, especially in conjunction with quantum chemical calculations of the complete tensor, provides details about electronic structure that are not observed when only the isotropic chemical shift is measured.<sup>19</sup> With the advent of the 2D techniques which separate the individual powder patterns of inequivalent carbons, especially the magic angle turning (MAT) method,<sup>20</sup> the complexity of systems that can be studied has greatly increased. In addition, due to advances in both computational methods and in available computer resources, quantum calculations are now feasible in these large systems. These advances have made it possible to obtain the anisotropic chemical shift data in systems such as the metallotetraphenylporphyrins.

In this paper the principal values of the  $^{15}\text{N}$  and the majority of the  $^{13}\text{C}$  chemical shift tensors present in the Zn, Mg, and Ni complexes of 5,10,15,20-tetraphenylporphyrin are presented along with DFT-GIAO calculations of the complete shift tensors

<sup>†</sup> Center for High Performance Computing.

<sup>‡</sup> Department of Chemical and Fuels Engineering.

<sup>⊗</sup> Abstract published in *Advance ACS Abstracts*, July 1, 1997.

(1) Smith, K. M. *Porphyrins and Metalloporphyrins*; Elsevier: Amsterdam, 1975.

(2) Schlabach, M.; Wehrle, B.; Rumpel, H.; Braun, J.; Scherer, G.; Limbach, H.-H. *Ber. Bunsenges. Phys. Chem.* **1992**, *96*, 821.

(3) Limbach, H.-H.; Hennig, J. *J. Am. Chem. Soc.* **1984**, *106*, 292.

(4) Stülbs, P. *J. Magn. Reson.* **1984**, *58*, 152.

(5) Braun, J.; Schlabach, M.; Wehrle, B.; Kocher, M.; Vogel, E.; Limbach, H.-H. *J. Am. Chem. Soc.* **1994**, *116*, 6593.

(6) Braun, J.; Limbach, H.-H.; Williams, P. G.; Morimoto, H.; Wemmer, D. E. *J. Am. Chem. Soc.* **1996**, *118*, 7231.

(7) Braun, J.; Schwesinger, R.; Williams, P. G.; Morimoto, H.; Wemmer, D. E.; Limbach, H.-H. *J. Am. Chem. Soc.* **1996**, *118*, 11101.

(8) Frydman, L.; Olivieri, A. C.; Diaz, L. E.; Frydman, B.; Morin, F. G.; Mayne, C. L.; Grant, D. M.; Adler, A. D. *J. Am. Chem. Soc.* **1988**, *110*, 336.

(9) Frydman, L.; Olivieri, A. C.; Diaz, L. E.; Valasinas, A.; Frydman, B. *J. Am. Chem. Soc.* **1988**, *110*, 5651.

(10) Frydman, L.; Olivieri, A. C.; Diaz, L. E.; Frydman, B.; Kustanovich, I.; Vega, S. *J. Am. Chem. Soc.* **1989**, *111*, 7001.

(11) Limbach, H.-H.; Hennig, J.; Kendricks, R.; Yannoni, C. S. *J. Am. Chem. Soc.* **1984**, *106*, 4059.

(12) Anderson-Altman, K. L. Ph.D. Thesis; University of Utah; 1994.

(13) Kawano, K.; Ozaki, Y.; Kyogoku, Y.; Ogoshi, H.; Sugimoto, H.; Yoshida, Z.-I. *J. Chem. Soc., Perkin Trans. 2* **1978**, 1319.

(14) Abraham, R. J.; Hawkes, G. E.; Smith, K. M. *J. Chem. Soc., Perkin Trans. 2* **1974**, 627.

(15) Abraham, R. J.; Hawkes, G. E.; Hudson, M. F.; Smith, K. M. *J. Chem. Soc. Perkin Trans. 2* **1975**, 204.

(16) Jakobsen, H. J.; Ellis, P. D.; Inners, R. R.; Jensen, C. F. *J. Am. Chem. Soc.* **1982**, *104*, 7442.

(17) Dominquez, D. D. Ph.D. Thesis; University of Washington; 1979.

(18) Gust, D.; Neal, D. N. *J. Chem. Soc., Chem. Commun.* **1978**, 681.

(19) Facelli, J. C. In *Encyclopedia of Nuclear Magnetic Resonance*; Grant, D. M., Harris, R. K., Eds; John Wiley: London, 1996; p 4327.

(20) Gan, Z. *J. Am. Chem. Soc.* **1992**, *114*, 8307.

in free base porphyrin and its Ca, Zn, Mg, and Ni complexes. The influence of the metal on the chemical shift values is discussed.

## Experimental Section

**Synthesis.** The  $^{15}\text{N}$ -labeled pyrrole was received from Cambridge Isotope Laboratory and used without further purification.<sup>21</sup> Thin layer chromatography (TLC) was performed on silica gel from Whatman (AL SIL G/UV) with  $\text{CHCl}_3$ /petroleum ether (3:1) as eluent. Larger amounts (1.2–1.5 g) of unlabeled metalloporphyrins were synthesized from commercial  $\text{H}_2\text{TPP}$ , obtained from Aldrich Chemical Company, following the identical procedure described below for the labeled compounds.

**5,10,15,20-Tetraphenylporphyrin- $^{15}\text{N}_4$ .**<sup>22–25</sup> A 1 mL amount of  $^{15}\text{N}$ -labeled pyrrole (14 mmol) and 1.5 mL of benzaldehyde (14 mmol) were dissolved in 1 L of dry  $\text{CH}_2\text{Cl}_2$  and stirred under nitrogen for 15 min at room temperature. Then 0.45 mL of 2.5 M  $\text{BF}_3$  in diethyl ether was added to the clear solution while shielding the reaction from ambient lighting. The solution turned dark red immediately. After 90 min, 2.75 g of *p*-chloranil was added, and the reaction vessel was immersed into a 45 °C preheated water bath and refluxed for 80 min. The solution was concentrated by rotary evaporation to ca. 100 mL, mixed with 12 g of Florisil (100–200 mesh) and evaporated to dryness. The dark powder was poured on top of a column of 2.5 cm diameter dry packed with ca 20 cm of Florisil (100–200 mesh) and eluted with 500 mL of  $\text{CH}_2\text{Cl}_2$ /petroleum ether (1:1) to give fraction 1. Further elution with  $\text{CH}_2\text{Cl}_2$  gave fraction 2 and 3. After evaporating the solvent the fractions yielded still impure  $\text{H}_2\text{TPP}$ . Fraction 1 yielded 476 mg; fraction 2, 661 mg; and fraction 3, 76 mg. The portion of  $\text{H}_2\text{TPP}$  used in the Zn and Ni metalation reactions was not purified further. The remaining  $\text{H}_2\text{TPP}$  was recrystallized from a methanol/chloroform solution by slowly evaporating  $\text{CHCl}_3$  from the  $\text{H}_2\text{TPP}$  and adding methanol.  $^1\text{H-NMR}$  (399.9 MHz):  $\delta$  (ppm) = 8.84 (s, 8 H, meso-H), 8.22 (q, 8 H, *o*-phenyl), 7.76 (m, 12 H, *m,p*-phenyl).  $^{13}\text{C-NMR}$  (100.64 MHz;  $\text{CDCl}_3$ ):  $\delta$  (ppm) = 120.20 (q, meso-C); 126.75 (t, meta-C); 127.78 (t, para-C); 131 (broad,  $\beta$ -pyrrole-C), 134.63 (t, ortho-C), 142.22 (q, ipso-C), 145 (broad,  $\alpha$ -pyrrole-C). CI-MS [ $m/z$  (%): 619 ( $\text{M}^+$ , 74.04), 647 ( $\Delta = 28$ ,  $+\text{CH}_2\text{CH}_3^+$ , 4.69).

**Zinc 5,10,15,20-Tetraphenylporphyrin- $^{15}\text{N}_4$ .**<sup>1</sup> A 200 mg amount of the impure  $^{15}\text{N}$ -labeled  $\text{H}_2\text{TPP}$  (0.33 mmol) was dissolved in 40 mL of  $\text{CHCl}_3$ , and 1 mL of saturated  $\text{ZnAc}_2$  in methanol solution was added. The solution was refluxed for 2 h and monitored by TLC. During rotary evaporation of the solution, methanol was gradually added to exchange the  $\text{CHCl}_3$  with methanol. When all the  $\text{CHCl}_3$  was exchanged with methanol, purple crystals were collected to yield 100 mg of  $^{15}\text{N}$ -labeled ZnTPP.  $^1\text{H-NMR}$  (399.9 MHz,  $\text{CDCl}_3$ ):  $\delta$  (ppm) = 8.95 (s, 8 H, meso-H), 8.22 (q, 8 H, *o*-phenyl), 7.77 (m, 12 H, *m,p*-phenyl).  $^{13}\text{C-NMR}$  (125.64 MHz;  $\text{CDCl}_3$ ):  $\delta$  (ppm) = 121.15 (q, meso-C), 126.52 (t, meta-C), 127.48 (t, para-C), 131.97 (t,  $\beta$ -pyrrole-C), 134.40 (t, ortho-C), 143.81 (q, ipso-C), 150.25 (q,  $\alpha$ -pyrrole-C). CI-MS [ $m/z$  (%): 681 ( $\text{M}^+$ , 100), 709 ( $\Delta = 28$ ,  $+\text{CH}_2\text{CH}_3^+$ , 5.86).

**Nickel(II) 5,10,15,20-Tetraphenylporphyrin- $^{15}\text{N}_4$ .**<sup>1</sup> A 200 mg amount of the impure  $^{15}\text{N}$ -labeled  $\text{H}_2\text{TPP}$  (0.33 mmol) was dissolved in 40 mL of  $\text{CHCl}_3$ , and 7 mL of saturated  $\text{NiAc}_2$  in methanol solution was added. The solution was refluxed for 5 days. The reaction was monitored by TLC. During rotary evaporation of the  $\text{CHCl}_3$  solution, methanol was gradually added. From the methanol solution a blue powder precipitated. When all  $\text{CHCl}_3$  had been exchanged with methanol the blue powder was collected to yield 110 mg of  $^{15}\text{N}$ -labeled NiTPP.  $^1\text{H-NMR}$  (399.9 MHz):  $\delta$  (ppm) = 8.74 (s, 8 H, meso-H), 8.01 (q, 8 H, *o*-phenyl), 7.68 (m, 12 H, *m,p*-phenyl).  $^{13}\text{C-NMR}$  (125.64 MHz;  $\text{CDCl}_3$ ):  $\delta$  = 118.99 (q, meso-C), 126.87 (t, meta-C), 127.74 (t,

para-C), 132.17 (t,  $\beta$ -pyrrole-C), 133.72 (t, ortho-C), 140.97 (q, ipso-C), 142.71 (q,  $\alpha$ -pyrrole-C). CI-MS [ $m/z$  (%): 575 ( $\text{M}^+$ , 100), 603 ( $\Delta = 28$ ,  $+\text{CH}_2\text{CH}_3^+$ , 5.86).

**Magnesium 5,10,15,20-Tetraphenylporphyrin- $^{15}\text{N}_4$ .**<sup>1,26</sup> A 110 mg amount of pure  $^{15}\text{N}$ -labeled  $\text{H}_2\text{TPP}$  (0.18 mmol) and 1 g of  $\text{MgClO}_4$  were dissolved in 25 mL of pyridine and refluxed overnight. After the reaction solution was cooled, the precipitate was filtered off and washed with diethyl ether until the filtrate was colorless. The magenta ether/pyridine phase was washed three times with 100 mL of distilled water, dried over  $\text{Na}_2\text{SO}_4$ , and rotary evaporated. The violet compound was then placed under high vacuum at 130 °C for two days to remove the pyridine coordinated to the MgTPP. Yield: 90 mg (79%).  $^{13}\text{C-NMR}$  (125.64 MHz;  $\text{CDCl}_3$ ):  $\delta$  (ppm) = 121.65 (q, meso-C), 126.24 (t, meta-C), 127.07 (t, para-C), 131.83 (t,  $\beta$ -pyrrole-C), 134.70 (t, ortho-C), 143.84 (q, ipso-C), 150.02 (q,  $\alpha$ -pyrrole-C). CI-MS [ $m/z$  (%): 641 ( $\text{M}^+$ , 100), 669 ( $\Delta = 28$ ,  $+\text{CH}_2\text{CH}_3^+$ , 5.86).

**Solid State Spectroscopy.** The solid state NMR measurements were made at room temperature on a Varian VXR-200 spectrometer system, with a  $^{15}\text{N}$  frequency of 20.279 MHz and a  $^{13}\text{C}$  frequency of 50.318 MHz. The CP/MAS and the  $^{15}\text{N}$  static experiments were performed using a 7 mm high speed variable temperature probe from Doty Scientific, Inc. The  $^{15}\text{N}$  spectra were recorded at room temperature using cross polarization with a 15 ms contact time and a proton 90° pulse of about 7  $\mu\text{s}$ . All  $^{15}\text{N}$  spectra were recorded using the  $^{15}\text{N}$ -enriched materials.

The  $^{13}\text{C}$  MAT experiments<sup>20,27,28</sup> were performed on the natural abundance nitrogen tetraphenylporphyrin samples, as insufficient quantities of the  $^{15}\text{N}$ -enriched material were available so that the MAT spectra could be obtained in a reasonable amount of time. A home built low speed spinning large volume (1.5  $\text{cm}^3$ ) probe<sup>29</sup> with a feedback loop to synchronize the pulse sequence to the rotor position was used.<sup>28</sup> A triple-echo MAT pulse sequence<sup>27</sup> with flip back, to allow shorter delay times, was used. The following experimental conditions were used: spinning rate about 16 Hz, spectral width in the acquisition dimension of 30 kHz, recycle time of 2 s, 90° proton pulse of 4.7  $\mu\text{s}$ , contact time of 4 to 5 ms, spectral width in the evolution dimension of 10 kHz (5 kHz for NiTPP), 800 scans per increment (1024 for NiTPP), and 37 complex 2D increments (28 for NiTPP). The 2D spectra were processed and sheared on a VAXstation 3100. When possible the powder pattern of each individual isotropic shift was obtained and fitted using a least squares fitting routine with the POWDER<sup>30</sup> approach; otherwise, the principal values were determined by visual comparison of the simulated spectral line shape to the experimental pattern. The  $C_\alpha$  patterns were fit on a IBM RS6000 computer using a POWDER-based fitting routine which accounts for the dipolar coupling to the  $^{14}\text{N}$ .

The literature  $^{13}\text{C}$  solution assignments for ZnTPP were confirmed by performing a 2D INADEQUATE experiment. The spectrum was analyzed using the FRED<sup>31</sup> software. Since the  $^{13}\text{C}$  spectra were similar for all the metallotetraphenylporphyrins, proton-coupled  $^{13}\text{C}$  experiments were sufficient to make unambiguous assignments for the other compounds. These experiments were performed on a Varian UnityPlus 500 MHz spectrometer system. As the metallotetraphenylporphyrins are only slightly soluble, the experiments were performed on a 10 mm broadband probe with a 24  $\mu\text{s}$  90° pulse in the carbon channel. The 2D INADEQUATE had a 4.0 kHz spectral width in both the acquisition and double quantum evolution dimension and was optimized to detect carbon-carbon bonds with a  $J_{\text{cc}}$  of 60 Hz. A total of 40 increments, with 800 scans per increment, were recorded. The acquisition time was 1.5 s and the delay time 4.5 s.

**Quantum Chemical Calculations.** DFT (Density Functional Theory) calculations were performed with the Gaussian 94 computer

(26) Baum, S. J.; Burnham, B. F.; Plane, R. A. *Proc. Nat. Acad. Sci. U.S.A.* **1964**, *52*, 1439.

(27) Hu, J. Z.; Orendt, A. M.; Alderman, D. W.; Pugmire, R. J.; Ye, C.; Grant, D. M. *Solid State NMR* **1994**, *3*, 181.

(28) Hu, J. Z.; Wang, W.; Liu, F.; Solum, M. S.; Alderman, D. W.; Pugmire, R. J.; Grant, D. M. *J. Magn. Reson. Ser. A* **1995**, *113*, 210.

(29) Jiang, Y. J.; Pugmire, R. J.; Grant, D. M. Manuscript in preparation.

(30) Solum, M. S.; Alderman, D. W.; Grant, D. M. *J. Chem. Phys.* **1986**, *84*, 3717.

(31) CBOND program. Varian, Palo Alto, CA. CCBOND is marketed by Varian as part of the Full Reduction of Entire Datasets (FRED) software.

(21) The commercial pyrrole was brown but could not be distilled because of the small amount. By using the impure material, the yield was decreased.

(22) Lindsay, J. S.; Wagner, R. W. *J. Org. Chem.* **1989**, *54*, 828.

(23) Wagner, R. W.; Lawrence, D. S.; Lindsay, J. S. *Tetrahedron Lett.* **1987**, *28*, 3069.

(24) Lindsay, J. S.; Hsu, H. C.; Schreiman, I. C.; Kearney, P. C.; Marguerettaz, A. M. *J. Org. Chem.* **1987**, *52*, 827.

(25) During work on this synthesis a more recent approach appeared in the literature. Gradillas, A.; del Campo, C.; Sinisterra, J. V.; Llama, E. F. *J. Chem. Soc., Perkin Trans. 1* **1995**, 2611.

program.<sup>32</sup> All calculations employed the GIAO<sup>33</sup> (Gauge Invariant Atomic Orbitals) method with either the 3-21g Pople basis set<sup>34</sup> for all atoms or the D95 basis set,<sup>35</sup> for carbons, nitrogens, and hydrogens and the Los Alamos ECP plus DZ basis (LanL2DZ)<sup>36</sup> for the metals. Calculations with both basis sets were performed when possible. The DFT calculations use the BLYP exchange correlation functional<sup>37,38</sup> and a coupled perturbative scheme without including the magnetic field effects in the exchange correlation functional.<sup>39</sup> The calculated <sup>15</sup>N chemical shieldings were converted to the shift scale by subtracting the absolute shielding value of nitromethane, -135.8 ppm.<sup>40</sup> The calculated <sup>13</sup>C chemical shieldings were converted to the TMS shift scale by subtracting the TMS shielding values of 186.7 and 193.6 ppm for the D95/LanL2DZ and 3-21g basis sets, respectively. These values were estimated from the corresponding calculated values for methane, 193.7 and 200.6 ppm, respectively, minus the 7 ppm difference between the chemical shieldings of TMS and methane reported in the literature.<sup>41</sup>

Geometry optimizations on the metal-TPP complexes using the D95/LanL2DZ basis set were not feasible with the available computer resources, and only the ZnTPP has a known molecular structure.<sup>42</sup> This room temperature X-ray structure predicts two very different Zn-N distances (2.045 and 2.029 Å), which, according to the calculations (see below), should lead to two very different <sup>15</sup>N isotropic chemical shifts. However, there is no NMR experimental evidence to support this nonequivalence. The very sharp features observed in the <sup>15</sup>N NMR spectra (both CP/MAS and static pattern) of ZnTPP indicate that any nonequivalence in both the isotropic and the principal values of the tensor should be less than 3 ppm. In addition, a <sup>15</sup>N CP/MAS spectrum recorded at about -90 °C shows no splitting, ruling out the possibility that some type of dynamic averaging is occurring in the room temperature spectrum. A powder diffraction taken on the ZnTPP sample used for the NMR measurements indicates that the sample is highly crystalline; however, the pattern lacks agreement with the literature X-ray data. One possible explanation for these discrepancies between the NMR and X-ray results may be that the NMR studies were done on a different crystal form than the X-ray study. Further studies are necessary to explore this suggestion. It should be noted that polymorphism has been previously observed in other porphyrins, and specifically in the free base TPP.<sup>43,44</sup> Fortunately, as will be seen in the following discussion, the DFT-optimized structures of the metal porphyrin complexes<sup>45</sup> that exist in the literature can be used to obtain information consistent with the experimental observations. The experimental ZnTPP geometry is only used in the calculations necessary to explore the effect of including the phenyl groups in the TPP ring on the calculated nitrogen chemical shift tensor.

A series of preliminary calculations were performed using the experimental geometry of the ZnTPP, in order to test the importance

(32) Gaussian 94 (Revision A.1), Frisch, M. J.; Trucks, G. W.; Schlegel, H. B.; Gill, P. M. W.; Johnson, B. G.; Robb, M. A.; Cheeseman, J. R.; Keith, T. A.; Petersson, G. A.; Montgomery, J. A.; Raghavachari, K.; Al-Laham, M. A.; Zakrzewski, V. G.; Ortiz, J. V.; Foresman, J. B.; Cioslowski, J.; Stefanov, B. B.; Nanayakkara, A.; Challacombe, M.; Peng, C. Y.; Ayala, P. Y.; Chen, W.; Wong, M. W.; Andres, J. L.; Replogle, E. S.; Gomperts, R.; Martin, R. L.; Fox, D. J.; Binkley, J. S.; Defrees, D. J.; Baker, J.; Stewart, J. P.; Head-Gordon, M.; Gonzalez, C.; Pople, J. A. Gaussian, Inc., Pittsburgh, PA, 1995.

(33) Ditchfield, R. *Mol. Phys.* **1974**, *27*, 789.

(34) Pietro, W. J.; Francl, M. M.; Hehre, W. J.; Defrees, D. J.; Pople, J. A.; Binkley, J. S. *J. Am. Chem. Soc.* **1982**, *104*, 5039.

(35) Dunning, T. H.; Hay, P. J. In *Modern Theoretical Chemistry*; Schaefer, H. F., III, Ed.; Plenum: New York, 1977; p 1.

(36) Hay, P. J.; Wadt, W. R. *J. Chem. Phys.* **1985**, *82*, 270. Ibid. pp 284 and 299.

(37) Lee, C.; Yang, W.; Parr, R. G. *Phys. Rev.* **1988**, *B37*, 785.

(38) Becke, A. D. *Phys. Rev.* **1988**, *A38*, 3098.

(39) Cheeseman, J. R.; Trucks, G. W.; Keith, T. A.; Frisch, M. J. *J. Chem. Phys.* **1996**, *104*, 5497.

(40) Jameson, C. J.; Mason, J. In *Multinuclear NMR*; Mason, J., Ed.; Plenum: New York, 1987; p 56.

(41) Jameson, A. K.; Jameson, C. J. *Chem. Phys. Lett.* **1987**, *134*, 461.

(42) Scheidt, W. R.; Mondal, J. U.; Eigenbrot, C. W.; Adler, A.; Radonovich, L. J.; Hoard, J. L. *Inorg. Chem.* **1986**, *25*, 795.

(43) Silvers, S. J.; Tulinsky, A. *J. Am. Chem. Soc.* **1967**, *89*, 3331.

(44) Hamor, T. A.; Caughey, W. S.; Hoard, J. L. *J. Am. Chem. Soc.* **1965**, *87*, 2305.

(45) Matsuzawa, N.; Ata, M.; Dixon, D. A. *J. Phys. Chem.* **1995**, *99*, 7698.

**Table 1.** Comparison of Calculated <sup>15</sup>N Chemical Shift Tensor Principal Values for the Three Models<sup>a</sup>

model	$\delta_{11}$	$\delta_{22}$	$\delta_{33}$
ZnTPP N <sub>1</sub>	10	-181	-398
N <sub>2</sub>	-47	-178	-419
average of N <sub>1</sub> and N <sub>2</sub>	-19	-180	-409
ZnTMP N <sub>1</sub>	18	-179	-392
N <sub>2</sub>	-41	-177	-416
average of N <sub>1</sub> and N <sub>2</sub>	-12	-178	-404
ZnTHP N <sub>1</sub>	13	-179	-399
N <sub>2</sub>	-42	-178	-420
average of N <sub>1</sub> and N <sub>2</sub>	-15	-179	-410
experimental	-16	-124	-393

<sup>a</sup> Models used are described in text. Reported results are in ppm relative to nitromethane, as discussed in text.

of the inclusion of the phenyl rings in the calculations of the <sup>15</sup>N chemical shifts tensors. These calculations were done using the smaller 3-21g basis set for different molecular models constructed as follows. Model I, designated ZnTPP, was constructed by adding the necessary H atoms, at standard distances and angles from the positions of the heavy atoms given by the X-ray structure of ZnTPP. Model II, ZnTMP, was constructed by replacing the phenyl groups in the ZnTPP by methyl groups. Standard geometrical parameters were used to determine the position of and bond lengths within the methyl groups. Model III, ZnTHP, was built using the ZnTPP structure and replacing the phenyl groups by hydrogen atoms. By preserving the geometry of the metalloporphyrin core and changing only the meso substituents a set of calculations which depend only on the direct electronic substituent effects was produced.

The results (<sup>15</sup>N only) of this series of calculations are given in Table 1. In this table it is observed, as was mentioned above, that as a consequence of the lack of symmetry in the X-ray diffraction structure the calculations predict two nonequivalent nitrogens. It is also observed that the average values of the principal components are independent of the substituent at the meso position, with the substituent inducing variations of less than 5 ppm in any of the principal components. These small variations are almost within the experimental error of the measurements. Therefore, these results justify the use of the unsubstituted metalloporphyrins as model compounds to calculate the chemical shift tensors for comparison with the experimental values measured in the metal-TPP complexes. The use of the unsubstituted compounds has two important advantages: it becomes possible to use a better basis set in the calculations, and it is possible to use the already published optimized structures of these compounds. The calculations on the unsubstituted porphyrins have the disadvantage that no comparison can be made between the experimental and calculated chemical shift tensor data for the carbons, as sizable substituent effects are observed in these atoms. Nonetheless, these effects are nearly independent of the metal used in the complex, as will be shown in the results.

In this work, therefore, the previously published DFT-optimized structures<sup>45</sup> for the parent porphyrin and for the Ca-porphyrin, Zn-porphyrin, Mg-porphyrin, and Ni-porphyrin complexes are used. We have included calculations on Ca-porphyrin because of its metal-nitrogen distance, even though no experimental chemical shift data have been measured for this compound. The Ca-nitrogen distance is one of the longest, while the Zn-nitrogen and Mg-nitrogen distances are intermediate and the Ni-nitrogen is one of the shortest for the metal-porphyrin compounds. It is interesting to note that the major structural change that occurs in the porphyrin unit to allow for this shortening of the metal-nitrogen distance is a decrease in the C<sub>α</sub>-C<sub>meso</sub>-C<sub>α</sub> angle. In all cases the metal lies in the plane of the porphyrin ring.

## Results and Discussion

The atomic designations used are shown in Figure 1. Figure 2 contains the <sup>15</sup>N powder patterns obtained for each of the three metal-TPP complexes along with their best spectral fits. The <sup>13</sup>C MAS spectra of all three of the metal-TPP complexes labeled with the assignments are given in Figure 3, and Figure 4 shows the 1D slices obtained from the <sup>13</sup>C 2D MAT of NiTPP.

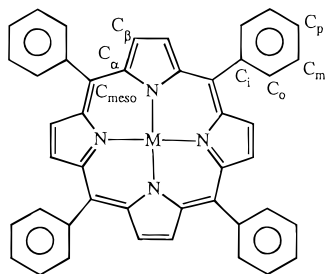


**Figure 1.** Structure of the metal complexes of 5,10,15,20-tetraphenylporphyrin, showing the labeling of the carbons used in this paper.

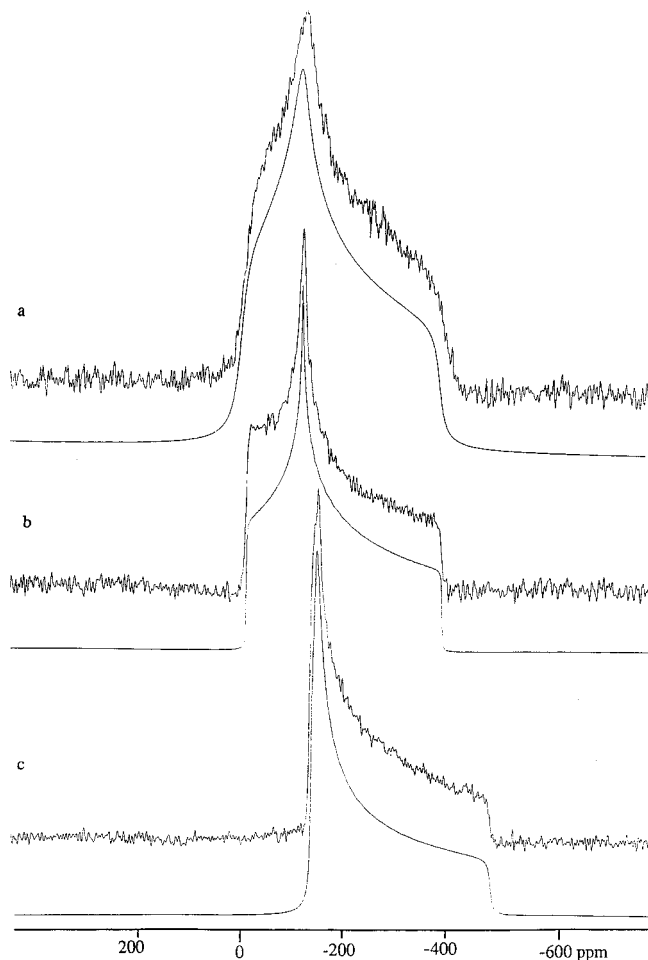


**Figure 2.** Experimental  $^{15}\text{N}$  powder patterns along with the best fit for (a) MgTPP, (b) ZnTPP, and (c) NiTPP.

**$^{15}\text{N}$  Chemical Shifts.** The resultant principal values of the chemical shift tensors are reported in Table 2, along with the tensor components for the nitrogens in the related species of pyrrole and the pyrrole anion.<sup>46</sup> As may be seen from the table, the principal values are nearly identical for the Mg and Zn, and these values are similar to those obtained for the pyrrole anion. The values obtained for the NiTPP are very different from those in the Mg- and ZnTPP, but are similar to the values measured for the nitrogen in the parent pyrrole, with an exception for a large difference between the  $\delta_{33}$  values.

The principal values reflect the change in the bonding present between the metal and the porphyrin ring. The similarity of both the isotropic chemical shift and the principal values of the chemical shift tensor for the Mg and Zn complexes is not too surprising as the 2+ ions of both have a closed outer shell, with

(46) Solum, M. S.; Anderson-Altmann, K. L.; Strohmeier, M.; Berges, D. A.; Zhang, Y.; Facelli, J. C.; Pugmire, R. J.; Grant, D. M., *J. Am. Chem. Soc.*, in press.

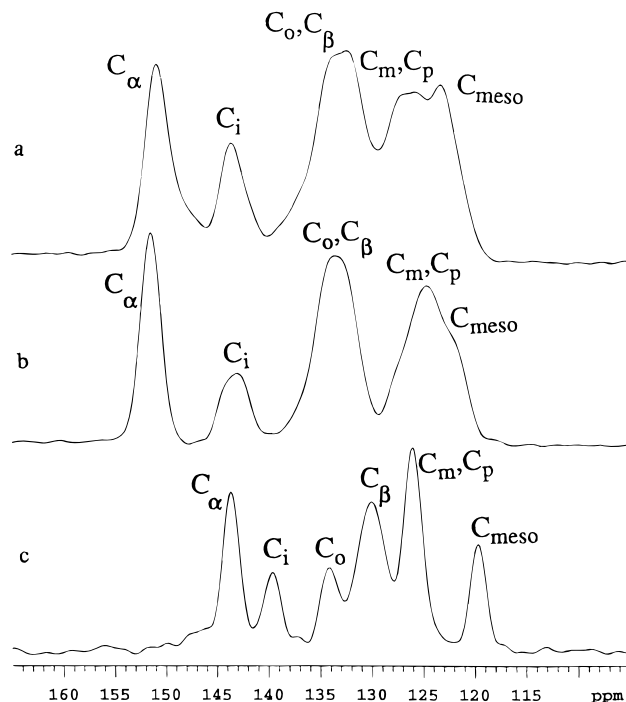


**Figure 3.**  $^{13}\text{C}$  CP/MAS spectra for (a) MgTPP, (b) ZnTPP, and (c) NiTPP. Assignments of the different resonances are indicated.

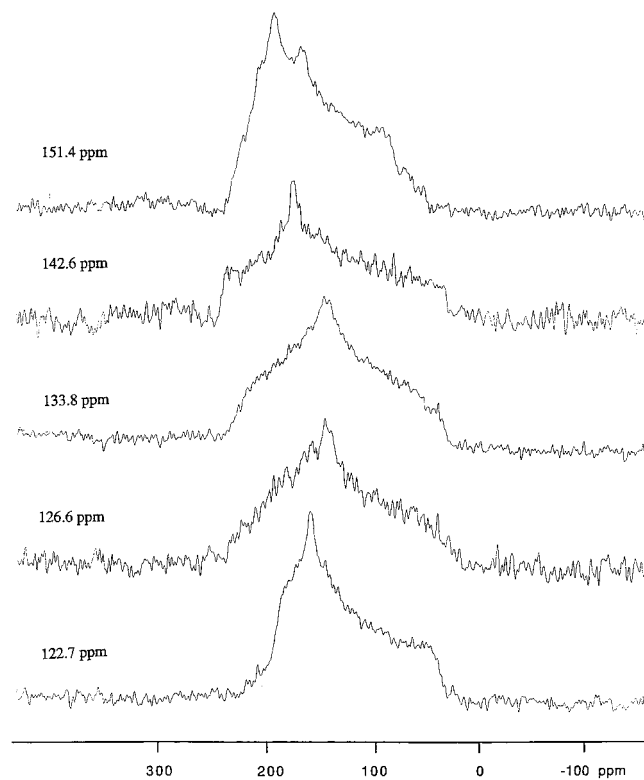


**Figure 4.** Slices taken from the 2D MAT spectrum of ZnTPP. The isotropic chemical shift of each slice is listed.

the  $\text{Mg}^{2+}$  having a  $s^2p^6$  electronic configuration and the  $\text{Zn}^{2+}$  a  $d^{10}$  electronic configuration.  $\text{Ni}^{2+}$ , on the other hand, has a  $d^8$  electronic configuration, which allows for the formation of a much stronger coordination bond between the TPP nitrogen and the nickel. In addition, the interaction between the metal and nitrogen has more covalent nature in NiTPP than in either Zn- or MgTPP, and in the NiTPP there also exists a substantial amount of backbonding from the metal to the porphyrin ring. The large shift observed in the  $\delta_{33}$  component in NiTPP is

**Table 2.** Experimental  $^{15}\text{N}$  Chemical Shift Tensor Principal Values of the Metal–TPP Complexes and Related Compounds<sup>a</sup>

compound	$\delta_{11}$	$\delta_{22}$	$\delta_{33}$	$\delta_{\text{iso}}$	$\delta_{\text{CP/MAS}}$	$\delta_{\text{soln}}$
ZnTPP	-16	-124	-393	-178	-178	-180.5
MgTPP	-10	-118	-392	-173	-179	-177.6
NiTPP	-136	-152	-478	-255	-254	-253.7
pyrrole anion <sup>b</sup>	-39	-90	-372	-167		
pyrrole <sup>b</sup>	-136	-234	-328	-233		

<sup>a</sup> All measurements were done on  $^{15}\text{N}$  enriched samples. The chemical shifts are reported in ppm relative to nitromethane. <sup>b</sup> Values taken from reference 46.

**Table 3.** Calculated  $^{15}\text{N}$  Chemical Shift Tensor Principal Values for Porphyrin and Metal–Porphyrin Complexes<sup>a</sup>

compound	R-(Me–N), <sup>b</sup> Å	$\delta_{11}$	$\delta_{22}$	$\delta_{33}$
porphyrin, N–H		-218, -170 ( $\delta_t$ )	-248, -202	-381, -354
porphyrin, N		20, 103 ( $\delta_t$ )	-147, -91	-423, -404
Ca–porphyrin	2.173	-61, 31 ( $\delta_t$ )	-182, -139	-405, -384
Mg–porphyrin	2.045	-90, -13 ( $\delta_t$ )	-178, -127	-406, -397
Zn–porphyrin	2.028	-69, 5 ( $\delta_t$ )	-178, -127	-404, -391
Ni–porphyrin <sup>c</sup>	1.953	-156, - ( $\delta_t$ )	-162, -	-422, -

<sup>a</sup> Values correspond to the 3-21g, D95/LanL2DZ basis set results, respectively. The components are given in rank order.  $\delta_{33}$  is always perpendicular to the molecular plane and the orientation of  $\delta_{11}$  predicted by the calculations at both basis set levels is given in parentheses. <sup>b</sup> Optimized metal–nitrogen distances taken from reference 45. <sup>c</sup> Calculations using the D95/LanL2DZ basis set did not converge in Ni–porphyrin; the spatial assignment reported is based on the 3-21g calculations (see text).

probably a direct consequence of this bonding interaction placing a higher electron density at the nitrogen. However, before discussing the effect of the different metals on tensor components it becomes necessary to rely on the calculations, in order to gain the information about the spatial orientation of the principal values.

The results of *ab initio* calculations of the chemical shift tensor are reported in Table 3. The  $\delta_{33}$  component is found to lie perpendicular to the plane of the porphyrin system, as is always the case in aromatic systems. The other two components which lie in the plane are designated the tangential component ( $\delta_t$ ), lying perpendicular to the metal–nitrogen bond, and the radial component ( $\delta_r$ ), lying along this bond. It is apparent that when the D95/LanL2DZ basis set is used in the calculations, the agreement between the calculated and experimental values is improved over the calculations using the 3-21g basis. With the larger basis set the agreement is such that there are no ambiguities in the spatial assignments of the principal components. Unfortunately, the calculation in Ni–porphyrin with the D95/LanL2DZ basis would not converge, so only the chemical shift values calculated at the 3-21g basis set level are available. In this case the larger error in the 3-21g basis set calculations coupled with the small difference between the two in-plane shift components renders the assignment of these orientations tentative for Ni–porphyrin. In spite of this problem, it is apparent from the table that as the strength of the bonding between the metal and the porphyrin ligand increases, as indicated by a shortened metal–nitrogen distance, the  $^{15}\text{N}$  chemical shift tensors move from the characteristic 5n type nitrogen (as in the pyrrole anion) to the 5p type nitrogen (in pyrrole), not only in the value of the tensor components but also in the orientation of these components.<sup>46</sup> The tangential component is the component undergoing large changes. The crossover of the  $\delta_t$  and  $\delta_r$  components is expected at a metal–nitrogen length of about 1.95 Å, which is close to the value for the Ni–porphyrin.

**Table 4.**  $^{13}\text{C}$  Chemical Shift Tensor Principal Values for Metal–TPP Complexes<sup>a</sup>

carbon	$\delta_{11}$	$\delta_{22}$	$\delta_{33}$	$\delta_{\text{iso}}$	$\delta_{\text{CP/MAS}}$	$\delta_{\text{liq}}$
NiTPP						
$\text{C}_\alpha$					143.6	142.7
$\text{C}_i$	236	156	24	139	139.6	140.9
$\text{C}_o$	215	147	30	131	134.0	133.7
$\text{C}_\beta$	217	141	24	127	130.0	132.2
$\text{C}_{\text{m,p}}$					126.0	m: 127.7 p: 126.9
$\text{C}_{\text{meso}}$	185	149	33	122	119.7	118.9
MgTPP						
$\text{C}_\alpha$					150.4	149.9
$\text{C}_i$	231	162	27	140	143.2	143.7
$\text{C}_{o,\beta}$					132.6	o: 134.7 $\beta$ : 131.8
$\text{C}_{\text{m,p}}$					125.8	m: 127.0 p: 126.2
$\text{C}_{\text{meso}}$	185	150	33	123	123.2	121.6
ZnTPP						
$\text{C}_\alpha$	208	188	59		151.4	150.2
$\text{C}_i$	233	166	23	141	142.6	142.8
$\text{C}_{o,\beta}$ <sup>b</sup>	209	137	48	131	133.8	o: 134.4 $\beta$ : 132.0
	224	144	27	132		m: 127.5 p: 126.5
$\text{C}_{\text{m,p}}$					126.6	
$\text{C}_{\text{meso}}$	186	152	31	123	122.7	121.1

<sup>a</sup> All chemical shifts obtained from the slices of 2D MAT spectra of the natural abundance nitrogen samples, as described in the text, and are reported in ppm relative to TMS. <sup>b</sup> There is no basis for making the assignment between these two carbons.

As discussed previously,<sup>46</sup> the  $\delta_r$  component is quite insensitive to the metal bonding even though large changes occur in the  $\delta_t$  component. These changes in  $\delta_t$  may be rationalized by an increase in the energy gap between the nitrogen lone pair (n) and  $\pi^*$  orbitals. The symmetry of this pair of orbitals is such as to dominate the value of  $\delta_t$ . When a bond is formed with the unpaired electrons of the nitrogen atom, the energy separation is increased appreciably. This behavior is similar to that observed in a series of nitrogen heterocycles.<sup>46</sup> Finally, it is important to emphasize that the metal–nitrogen separation is the most relevant factor in determining the  $^{15}\text{N}$  chemical shift tensor. Note, the tensors in Mg–porphyrin and Zn–porphyrin are quite similar, and their metal–nitrogen distances are also comparable.

**$^{13}\text{C}$  Chemical Shifts.** The principal values of the  $^{13}\text{C}$  chemical shift tensors obtained using the MAT experiment are reported in Table 4. The assignments of the chemical shifts in the solution were made by recording an INADEQUATE spectrum on the ZnTPP. Unfortunately, neither NiTPP nor MgTPP were soluble enough to obtain an INADEQUATE spectrum; therefore, the assignments were made by a comparison of the  $^{13}\text{C}$ – $^1\text{H}$  *J*-coupling patterns of the two compounds with that measured in the ZnTPP. The solid state chemical shift assignments are based on comparison of solution and solid state isotropic chemical shifts. Due to the high degree of signal overlap, as may be observed in the MAS spectra in Figure 3, it was not possible to obtain all of the chemical shift tensor data for all of the carbons.

Unfortunately, at this time a comparison cannot be made between the metallotetraphenylporphyrins and  $\text{H}_2\text{TPP}$ , due to the increased number of resonances in  $\text{H}_2\text{TPP}$  because of its lower molecular symmetry and the additional complication of the dynamic rearrangement of the two inner hydrogens. In addition, the dynamics of the hydrogen rearrangement in the free base TPP is complicated by two crystalline forms.<sup>40,41</sup> The dynamic process of the hydrogen rearrangement has previously been studied by variable temperature  $^{15}\text{N}$  CP/MAS NMR in both

**Table 5.** Calculation of  $^{13}\text{C}$  Chemical Shift Tensors Principal Values of Porphyrin and Several Metal–Porphyrin Complexes<sup>a</sup>

compound	$C_\alpha$			$C_\beta$			$C_{\text{meso}}$		
	$\delta_{11}$	$\delta_{22}$	$\delta_{33}$	$\delta_{11}$	$\delta_{22}$	$\delta_{33}$	$\delta_{11}$	$\delta_{22}$	$\delta_{33}$
porphyrin	197	158	43	207	124	38			
N–H ring	165	130	33	174	109	32			
porphyrin	209	176	70	214	119	45			
N ring	177	147	56	180	106	39			
porphyrin	203	167	57	211	122	42	174	107	19
avg <sup>b</sup>	171	139	45	177	108	36	145	92	15
Ca–porphyrin	199	183	55	211	127	48	178	123	29
	168	154	44	178	115	41	151	107	23
Mg–porphyrin	202	183	55	212	125	47	182	117	29
	171	153	44	178	110	40	152	99	23
Zn–porphyrin	203	182	54	212	124	47	181	116	28
	172	153	45	179	111	39	149	98	22
Ni–porphyrin	—	—	—	—	—	—	—	—	—
	181	147	37	180	112	42	152	87	26

<sup>a</sup> The first row of values correspond to results with the D95/LanL2DZ basis set and the second row to those with the 3-21g basis set. <sup>b</sup> All four meso carbons are the same.

the pure, triclinic form of free base TPP, as well as in the tetragonal form with a mixed crystal of the free base and a metal-complexed TPP.<sup>2,11</sup> It is not understood if the tetragonal form is only obtained in cases of impurities or mixed crystals, however. A direct comparison between the experimental and calculated  $^{13}\text{C}$  chemical shift tensor components is also not possible as the calculations were performed on the metal–porphyrin complexes instead of on the metal–TPP compounds, for the reasons presented in the section describing the quantum chemical calculations.

From the  $^{13}\text{C}$  MAS spectra in Figure 3 and isotropic chemical shifts given in Table 4 it may be seen that, except for  $C_\alpha$ , there is little change between the isotropic chemical shifts of three metal–TPP complexes. The largest change is a 7 ppm difference between the isotropic chemical shifts of the  $C_\alpha$  carbon in NiTPP as compared to either the Zn or Mg compounds. The remainder of the carbons have isotropic chemical shifts that agree to within 3 ppm between the three different metals. Again, the largest changes are observed between the Ni and either the Zn or Mg complexes, with the latter two having chemical shifts that differ by less than 1 ppm. Essentially, the effect of changing the metal center is isolated in the nitrogen chemical shifts.

From the data in Table 4 it is obvious that there are only minor changes in the principal values of the  $^{13}\text{C}$  chemical shift tensors as the metal is changed. Even though principal values could not be extracted from the slices for the *meta* and *para* carbons of the phenyl ring, the line shapes are essentially identical, indicating that no significant differences exist between the three metal complexes. In addition, the principal values obtained for the phenyl ring carbons are typical values for aromatic carbons, indicating that there is no interaction between the phenyl  $\pi$ -system and that of the porphyrin ring. This is expected as the angle between the plane of the porphyrin ring and that of the phenyl group, as measured by X-ray, does not allow for interaction between the two  $\pi$ -systems.<sup>42–44</sup> Among the porphyrin ring carbons, the variation of any shift component of a given carbon is less than 10 ppm among the three metal complexes.

The same conclusion is reached from the calculated components in the metalloporphyrins given in Table 5. The variations for a given carbon ( $C_\alpha$ ,  $C_\beta$ , or  $C_{\text{meso}}$ ) are all about 5 ppm or less. The only exception to this observation is the  $\delta_{22}$  component of  $C_{\text{meso}}$ , which decreases as the metal–nitrogen distance is decreased. However, the decrease of about 10 ppm

when replacing Ni by either Mg or Zn observed in the calculated chemical shift component is not observed in the experimental values. The lack of sensitivity of the  $^{13}\text{C}$  chemical shift to the metal substitution is observed in the calculations. The only large changes (on the order of 15 ppm) observed between the free base porphyrin and the metal–porphyrin complexes are in the  $\delta_{22}$  components of  $C_\alpha$  and  $C_{\text{meso}}$ .

The effect of the quadrupolar coupling constant of the  $^{14}\text{N}$  on the dipolar coupled spectrum of the  $C_\alpha$  carbon is observed in the  $C_\alpha$  slice of the MAT spectra. This provides an opportunity to obtain the axes of the  $C_\alpha$  principal values from the experiment by exploiting the spatial term in the quadrupolar coupling Hamiltonian. As the signal to noise ratio required to accurately fit dipolar patterns is high, only the  $C_\alpha$  pattern of the ZnTPP was possible to fit. However, the patterns for the NiTPP and the MgTPP possess the same features as that of the ZnTPP, indicating that the results discussed below can be applied to all three cases. The results of the spectral fitting gave the principal values reported in Table 4. It should be noted that the calculated values for  $C_\alpha$  of Zn–porphyrin agree with the experimental values in ZnTPP, indicating that the phenyl ring is too far away to effect the chemical shift components of this carbon. The spectral fitting determined that the dipolar coupling is 818 Hz, corresponding to a  $C_\alpha$ –N distance of 1.387 Å. No thermal corrections or anisotropy in the J coupling was included in the estimation of this distance.<sup>47</sup> This bond distance is in good agreement with both the experimental distance of 1.376 Å<sup>42</sup> and the optimized value (in Zn–porphyrin) of 1.369 Å.<sup>45</sup> The  $\delta_{33}$  component of the  $^{13}\text{C}$  chemical shift tensor for  $C_\alpha$  is found to be perpendicular to the plane of the porphyrin ring as expected, thereby restricting the remaining two components to lie in the plane of the porphyrin system. In addition, the  $\delta_{22}$  component was determined to lie in the pyrrole plane at an angle of 32° relative to the  $C_\alpha$ –N bond. This corresponds to an orientation of the  $\delta_{11}$  component for  $C_\alpha$  of either 10° from the  $C_\alpha$ – $C_\beta$  bond, oriented outside of the pyrrole ring, or 53° from the  $C_\alpha$ – $C_\beta$  bond, oriented inside of the pyrrole ring. These angles have an uncertainty of about 10°. The first of these two orientations is in reasonable agreement with the calculated orientation for the Zn–porphyrin, which is 19°, oriented outside of the pyrrole ring, with the D95/LanL2DZ basis set and 18° with the 3-21g basis set. The fit of the spectrum is fairly insensitive to the quadrupolar coupling constant of the  $^{14}\text{N}$  which is estimated as less than 5 MHz.

## Conclusions

In this paper the principal values of the  $^{15}\text{N}$  chemical shift tensors along with the majority of those of the  $^{13}\text{C}$  chemical shift tensors are reported for the Mg, Zn, and Ni complexes of 5,10,15,20-tetraphenylporphyrin. Calculations of the chemical shift tensor are also provided for the Ca, Mg, Zn, and Ni complexes of porphyrin. DFT-GIAO chemical shielding calculations using moderate or even small basis sets provide adequate results to interpret the experimental results for these large, complex molecular systems containing metals. It is shown that the calculations for the  $^{15}\text{N}$  chemical shift tensor are independent of the substituent at the meso position. In addition, the  $^{13}\text{C}$  chemical shift tensors were very similar for all of the compounds, both in the experimental and calculated data, with differences between the four metal complexes generally being less than 5 ppm. The only significant changes observed due to the presence of the different metals are in the nitrogen chemical shift tensor. These changes are very large, with differences of over 80 ppm measured in both the  $\delta_{11}$  and the  $\delta_{33}$  components.

(47) Zilm, K. W.; Grant, D. M. *J. Am. Chem. Soc.* **1981**, *103*, 2913.

The chemical shift tensor of the nitrogen changed from being similar to that observed in the pyrrole anion to being similar to that in pyrrole as the metal–nitrogen separation decreased. A change is also observed in the calculated orientation of the two in-plane components. Calculations on porphyrin complexes with longer metal–nitrogen distances indicate that the  $\delta_{11}$  component is tangential to the metal–nitrogen bond, and as the metal–nitrogen separation is decreased the two in-plane components become nearly degenerate and then crossover such that the  $\delta_{22}$  component becomes the tangential component. This crossover appears to occur at a metal–nitrogen separation of about 1.95 Å. This conclusion is also supported by the experimental data, as the two downfield components of the  $^{15}\text{N}$  chemical shift tensor measured for NiTPP, where the Ni–N distance is calculated to be 1.953 Å, are only separated by 22 ppm. In addition, ZnTPP and MgTPP have similar metal–nitrogen separations, and the measured principal values of the

$^{15}\text{N}$  chemical shift tensor of these two compounds are within experimental error of each other.

**Acknowledgment.** This work was funded in part by the National Institutes of Health from the Institute of General Medical Sciences through Grant GM08521-34. Funding for purchase of the  $^{15}\text{N}$ -labeled pyrrole was provided by a research and training grant from Exxon Corporation. Computational resources were provided by the Center for High Performance Computing at the University of Utah. Mark Strohmeier is grateful for a fellowship from the Technical University of Braunschweig, funded by the German Academic Exchange Service (DAAD), to come to the University of Utah. Special thanks are extended to Jamie Manson for obtaining the powder diffraction on the ZnTPP.

JA970447G